

This article was downloaded by:

On: 22 January 2011

Access details: *Access Details: Free Access*

Publisher *Taylor & Francis*

Informa Ltd Registered in England and Wales Registered Number: 1072954 Registered office: Mortimer House, 37-41 Mortimer Street, London W1T 3JH, UK



## The Journal of Adhesion

Publication details, including instructions for authors and subscription information:

<http://www.informaworld.com/smpp/title~content=t713453635>

### Degradation of Fatigue Properties of Weld-Bonded Aluminum Exposed to Moisture and Elevated Temperature

P. C. Wang<sup>a</sup>; P. Mabery<sup>b</sup>; C. K. Chisholm<sup>c</sup>

<sup>a</sup> Physics Department, Research and Development Center, General Motors Corporation, Warren, Michigan, USA <sup>b</sup> General Motors Corporation, Warren, Michigan, USA <sup>c</sup> Ford Motor Company, Dearborn, Michigan, USA

**To cite this Article** Wang, P. C. , Mabery, P. and Chisholm, C. K.(1993) 'Degradation of Fatigue Properties of Weld-Bonded Aluminum Exposed to Moisture and Elevated Temperature', *The Journal of Adhesion*, 43: 1, 121 – 137

**To link to this Article:** DOI: 10.1080/00218469308026592

**URL:** <http://dx.doi.org/10.1080/00218469308026592>

PLEASE SCROLL DOWN FOR ARTICLE

Full terms and conditions of use: <http://www.informaworld.com/terms-and-conditions-of-access.pdf>

This article may be used for research, teaching and private study purposes. Any substantial or systematic reproduction, re-distribution, re-selling, loan or sub-licensing, systematic supply or distribution in any form to anyone is expressly forbidden.

The publisher does not give any warranty express or implied or make any representation that the contents will be complete or accurate or up to date. The accuracy of any instructions, formulae and drug doses should be independently verified with primary sources. The publisher shall not be liable for any loss, actions, claims, proceedings, demand or costs or damages whatsoever or howsoever caused arising directly or indirectly in connection with or arising out of the use of this material.

# Degradation of Fatigue Properties of Weld-Bonded Aluminum Exposed to Moisture and Elevated Temperature

P. C. WANG

*Physics Department, Research and Development Center, General Motors Corporation, Warren, Michigan 48090-9055, USA*

P. MABERY

*General Motors Corporation, Warren, Michigan 48090-9010, USA*

C. K. CHISHOLM\*

*Ford Motor Company, Dearborn, Michigan 48121, USA*

*(Received April 5, 1993; in final form July 13, 1993)*

Experiments have been completed in order to characterize the fatigue behavior of weld-bonded aluminum 5754-O/bis-phenol-A epoxy adhesive joints subjected to 100% relative humidity at 38°C. It was found that the presence of water vapor at elevated temperature decreases the fatigue strength of weld-bonded joints by as much as 33% at  $5 \times 10^6$  cycles. Optical microscopy, scanning electron microscopy, dynamic mechanical analysis, and tensile testing of fatigued specimens and exposed bulk adhesive revealed that fatigue strength degradation is mainly due to the plasticization and micro-cracking of adhesive by the water vapor.

**KEY WORDS** weld-bonding aluminum; vehicle applications; moisture and elevated temperature; concurrent fatigue testing; fatigue strength; adhesive plasticization.

## INTRODUCTION

Weld-bonded (a combination of adhesive bonding and spot welding) aluminum is known to have good stiffness and strength combined with light weight, providing a potentially wide range of applications, especially in light-weight vehicle structures. Despite these advantages, the use of weld-bonded aluminum in vehicle structural applications has been limited, mainly because of concerns regarding environmental durability, particularly the effect of moisture. In order to utilize the full potential of weld-bonded aluminum, its durability performance at elevated temperature and at high moisture contents must be understood.

---

\*Formerly with General Motors Corporation

A number of studies have been published concerning the deleterious effects of salt spray<sup>1</sup> and service environment<sup>2</sup> on the durability of weld-bonded aluminum. However, to the best of our knowledge, most previous research on the corrosion fatigue properties of weld-bonded aluminum has been conducted on the specimens after environmental exposure. The degradation of the bond is often far less than the damage from concurrent corrosion fatigue testing in which corrosion and cyclic mechanical loading are involved simultaneously.<sup>3</sup> Since vehicles encounter various environment extremes during service loading, concurrent corrosion fatigue properties of weld-bonded aluminum are of considerable importance.

In this paper, the effect of moisture at elevated temperature on the fatigue strength of weld-bonded aluminum 5754-O is studied. Tests were conducted in essentially two environments: a 100% relative humidity (R.H.) at 38°C to simulate a "hot and humid" (hereafter referred to as wet) environment, and a 35% R.H. at 20°C to simulate the ambient (hereafter referred to as dry) environment. In doing this work, we have used lap-shear specimens made from aluminum 5754-O/bis-phenol-A epoxy adhesive. In addition to the optical and scanning electron microscopy (SEM), dynamic mechanical analysis (DMA) was employed to study the environmental failure mechanism. This investigation is part of a larger program to develop a more quantitative and predictable description of environmental corrosion fatigue.

## EXPERIMENTAL PROCEDURE

### Material

2.0 mm thick aluminum 5754-O was bonded with epoxy adhesive. The aluminum alloy was surface treated using a proprietary process. A mixture of silicon-chromium oxide was coated on the aluminum surface to prevent the aluminum oxide from forming during welding and to enhance the adhesion between adhesive and adherend. Nuclear magnetic resonance (NMR), Fourier transform infrared spectroscopy (FTIR), X-ray diffraction (XRD), polarized light microscopy, scanning electron (SEM) and transmission electron microscopy (TEM) analyses of the epoxy adhesive showed that it is composed of bis-phenol-A epoxy resin, fumed silica, quartz, and wollastonite (*i.e.*, CaSiO<sub>3</sub>).<sup>4</sup> The curing agent appears to be an amine compound.<sup>4</sup> Tensile properties of the aluminum 5754-O and bis-phenol-A epoxy adhesive are given in Tables I and II, respectively.

### Specimen Fabrication

The lap-shear specimens were fabricated from 25.4 × 175 mm coupons. Figure 1 shows the schematic of a lap-shear weld-bonded specimen. Specimens were prepared by: (1) applying the one-part, heat curing, toughened adhesive, through a hand-held injection gun, on one of the two contact surfaces; (2) bringing the adherends together; (3) positioning them with a fixture; (4) spot welding the specimens (A spot weld with a nugget diameter of 5 mm was centered on a 25.4

TABLE I  
Tensile properties\* of aluminum 5754-O

	Longitudinal	Transverse
0.2% Yield strength (MPa)	126	115
Tensile strength (MPa)	227	220
% Elongation (in 50.8 mm)	20.2	22.5
Strain hardening exponent, n	0.256	0.273

\*under a strain rate of  $3.3 \times 10^{-3}$ /sec.

TABLE II  
Tensile properties of the bis-phenol-A epoxy adhesive\*

Tensile modulus (GPa)	2.80
Tensile strength (MPa)	57.82
% Elongation at break	5.44

\*under a stroke rate of 0.01 mm/sec.

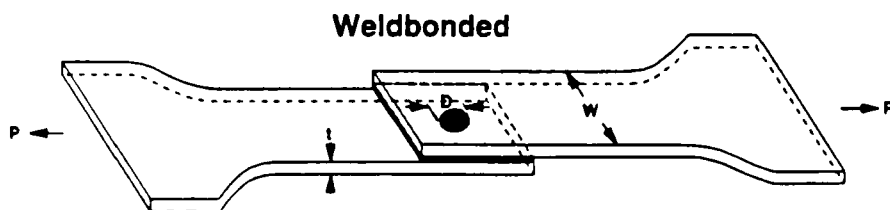


FIGURE 1 Schematic of a lap-shear weld-bonded joint.

TABLE III  
Welding parameters

Welding current (kA)	Welding time (cycle)*	Electrode force (lb)	Electrode force (N)	Electrode cap
22.7	8	600	2,669	MWZ 6008

\*1 cycle = 1/60 second.

mm square overlap region. The weld nugget was prepared using a single-phase, microprocessor-controlled AC electrical resistance welding unit. The welding schedule employed is given in Table III); and (5) curing the specimens through a two-stage process (*i.e.*, 10 minutes at 145°C for wetting the adherend, and then 30 minutes at 175°C for cross-linking). All finished specimens were examined for any defects. In order to reduce the scatter in the data, the specimens with defects (*i.e.*, uneven bondline thickness and pores at the adhesive fillet) were discarded.

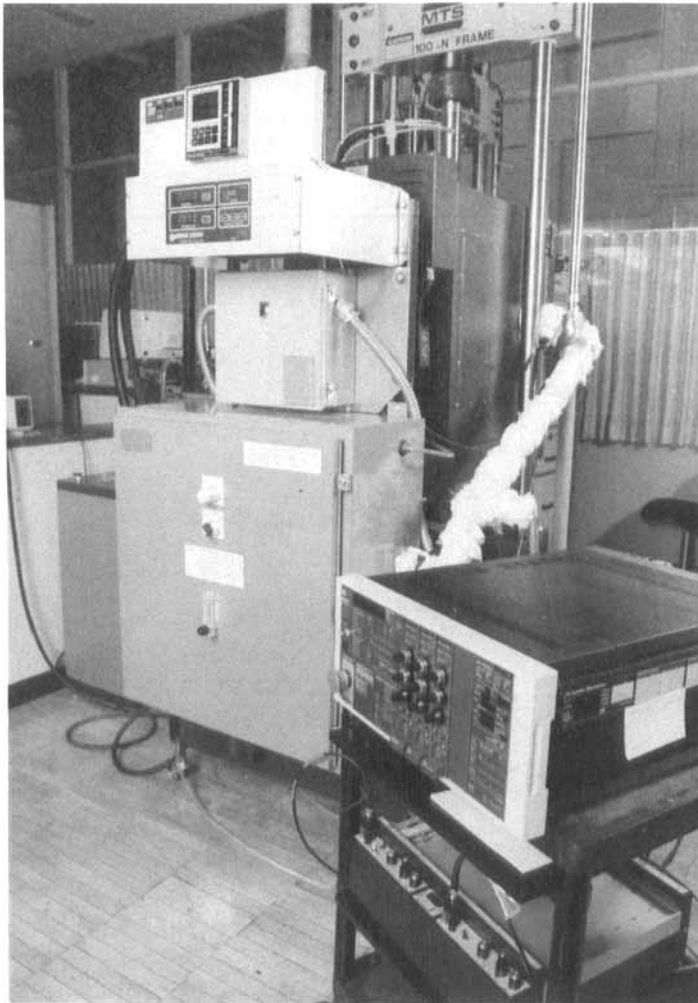


FIGURE 2 Photograph of the testing setup.

### **The Environmental Chamber**

The corrosion fatigue tests were performed in an environmental chamber. Figure 2 shows the whole testing setup including the test chamber, sampling system, moisture control system, humidifier, cooling system and fatigue testing machine. The water vapor was supplied through the humidifier. The vapor is added in the form of steam by boiling faucet water in a stainless steel tank maintained at a constant temperature. The steam flow is controlled by the output signal of the dew point controller. The vapor is pumped into the chamber and is circulated inside the chamber by means of a circulating fan (placed inside the chamber) to maintain a uniform envi-

ronment throughout the chamber. The relative humidity (R.H.) inside the chamber is controlled by means of an optical dew point hygrometer. Negligible condensation occurred during testing.

### Fatigue Testing

Specimens were gripped in self-aligning hydraulic grips. To minimize bending stresses during testing, both ends of the specimens were attached by adhesive to two filler plates of the same thickness. Since the moisture-temperature state requires some time to stabilize, all specimens remained in the environmental chamber (100% R.H. at 38°C) for 2 hours before the start of each test. Fatigue tests were conducted in the controlled relative humidity inside the environmental chamber. All fatigue tests were performed with a sinusoidal wave form at a frequency of 10 Hz and a stress ratio  $R = 0.1$  ( $R = \text{min}/\text{max load}$ ). Complete separation of the test piece into two pieces was defined as failure.

### Fractography

Post-failure fractographic analysis was performed with scanning electron microscopy to study the failure mechanisms for both dry and wet environments. Specimens were cut from the broken overlap sections. Before the SEM examination, each specimen was sputter-coated with gold-palladium.

### Measurement of Glass Transition Temperature

Essential to joint durability is the behavior of the cured adhesive under hygrothermal exposure. Thus, bulk adhesive properties (*i.e.*, glass transition temperatures) were determined by dynamic mechanical analysis (DMA).<sup>5</sup> This test was accomplished using a DuPont Model 982 DMA analyzer. Specimen dimensions were approximately  $30 \times 14.2 \times 3.8$  mm. The heating rate for the adhesive specimens was 3°C/min. Software was used to obtain the dynamic shear storage ( $G'$ ) and loss ( $G''$ ) moduli as functions of temperature. The glass transition temperature ( $T_g$ ) was defined as the temperature indicated by the main peak in the loss modulus ( $G''$ ).

Prior to DMA, the adhesive specimens were conditioned by exposure to either an ambient laboratory environment or environmental chamber. Moisture uptake during hygrothermal conditioning was determined by weight measurements. The moisture content is defined as:  $M = [(\text{weight of moist material} - \text{weight of dry material}) / \text{weight of dry material}] \times 100\%$ .

## RESULTS AND DISCUSSION

### Fatigue Test Results

Fatigue test results for weld-bonded specimens, obtained in dry (*i.e.*, ambient condition) and wet (*i.e.*, 100% humidity at 38°C) environments, are plotted in Figure 3. In order to determine whether moisture affects the fatigue strength of weld-bonded

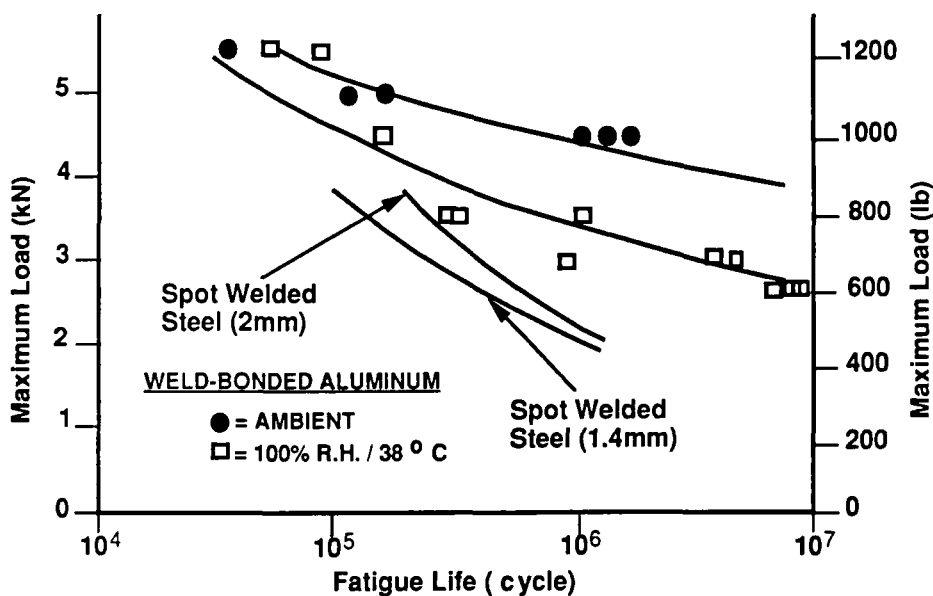


FIGURE 3 Fatigue test results for weld-bonded aluminum 5754-O joints in ambient and concurrent humidity and elevated temperature environments (Steel spot weld data are from Ref. 7).

aluminum, statistical analysis (F-test) was performed. Details of the F-test are described in Ref. 6, and will not be elaborated here. Statistical analyses showed that under a 95% confidence level, there is a significant difference between the two test conditions. A curve-fitting analysis was performed to obtain the load vs. life relationship for each case. As shown, no significant difference was found between the fatigue resistances at short lives ( $<10^5$  cycles). However, at long lives, weld-bonded joints are deteriorated substantially by heat and moisture. At  $5 \times 10^6$  cycles, the reduction of fatigue strength due to 100% R.H./38°C is about 33%. Because a low amplitude cyclic load results in a long test which allows time for interaction between material and environment, the differences are expected to become more pronounced in the high cycle regime.

For comparison purposes, fatigue data of spot-welded steel<sup>7</sup> with gauges of 2 mm and 1.4 mm are also included in Figure 3. The steel spot weld with 1.4 mm gauge was selected because Glaser *et al.*<sup>8</sup> found that similar static strengths can be achieved for spot-welded steel and weld-bonded aluminum alloy, where the aluminum sheet thickness is 1.4 times that of the steel. As shown, weld-bonded aluminum joints in 100% R.H./38°C were shown to out-perform the spot-welded steel. It should be noted that data reported here were obtained under a frequency of 10 Hz. Fatigue properties of spot-welded steel are insensitive to the testing frequency and wet environment used in this study. By contrast, fatigue properties of weld-bonded aluminum are frequency dependent. Preliminary test results showed that for an applied load range of 4.95 kN, reducing the loading frequency from the 10 Hz to 1 Hz produced a decrease in the fatigue life from  $6.6 \times 10^4$  to  $2.7 \times 10^4$  cycles. The

decrease in fatigue life is possibly a result of more time (*i.e.*, lower frequency) allowed for environmental attack during the fatigue process.

### Fractography

Comparison of the fatigue test data in Figure 3 shows a difference in fatigue strength between the dry and wet specimens. This may be due to the change in failure mode with the increase in moisture and temperature. Adherend-tearing and cohesive failure modes were observed for both dry and wet specimens. Figures 4(a) and 5(a) show the adherend-tearing failure mode for dry and wet specimens, respectively. Cracks initiated from the edge of the overlap, and grew across the adherend width. Finally, specimens failed by tensile overload of the remaining unseparated sections. However, preliminary visual examination of specimens with the cohesive failure mode revealed significant differences in the fracture appearance between the dry and wet environments. Fatigue failures in dry specimens were characterized by cracks that had initiated at the edge of the overlap, and then grew through the adhesive (Fig. 4(b)). Specimens failed by the coalescence of multiple microcracks at the edges of the weld nugget. A scanning electron micrograph of the fracture surface is shown in Fig. 4(c). As shown, the fracture surfaces consist of dark, randomly-shaped islands (region B) that are scattered unevenly on an otherwise gray background (region C). A closer examination of a typical island clearly reveals that the grey surface is adjacent to one aluminum/adhesive interface whereas the dark surface is near the other. As compared with the aluminum surface (region A), it clearly shows that the regions B and C are covered by adhesive. In contrast, the wet specimens were associated with cracks that appeared to propagate along the adherend-adhesive interface (Figs. 5(b) and 5(c)). However, careful examinations of Figure 5(c) showed that a very thin layer of adhesive sticks onto the aluminum substrate (see Fig. 5(d)). Laird<sup>9</sup> found that water diffusion along the adherend/polymer interface may be 450 times as fast as through the bulk polymer. The boundary layer of the adhesive near the adhesive/adherend has a high water absorption and, conceivably, could be more degraded than the bulk adhesive. As a result of this, the locus of failure was shifted from the adhesive layer to the interfacial region. A future effort should be to investigate if this near-interfacial failure may be the result of the stress directing the failure into the region near the interfacial area.

Based upon the fractography observations, it appeared that the cohesive failure mode often occurred in the low-to-medium-cycle regime, whereas the adherend-tearing failure mode became dominant at the high-cycle regime. This failure mode difference can be attributed to the local stress intensity. Finite element stress analyses of weld-bonded aluminum joint showed that at the edge of the overlap mode I stress is greater than mode II stress.<sup>10</sup> For a low applied load, a combination of mode I stress and the absence of a true fatigue limit for aluminum (*i.e.*, its inability to endure an infinite number of cycles without failure)<sup>11</sup> may lead to the cracks eventually initiating and propagating across the adherend width. For a high level applied load a severe mode II stress may exceed the threshold toughness of the adhesive and, therefore, the cohesive failure mode becomes dominant.



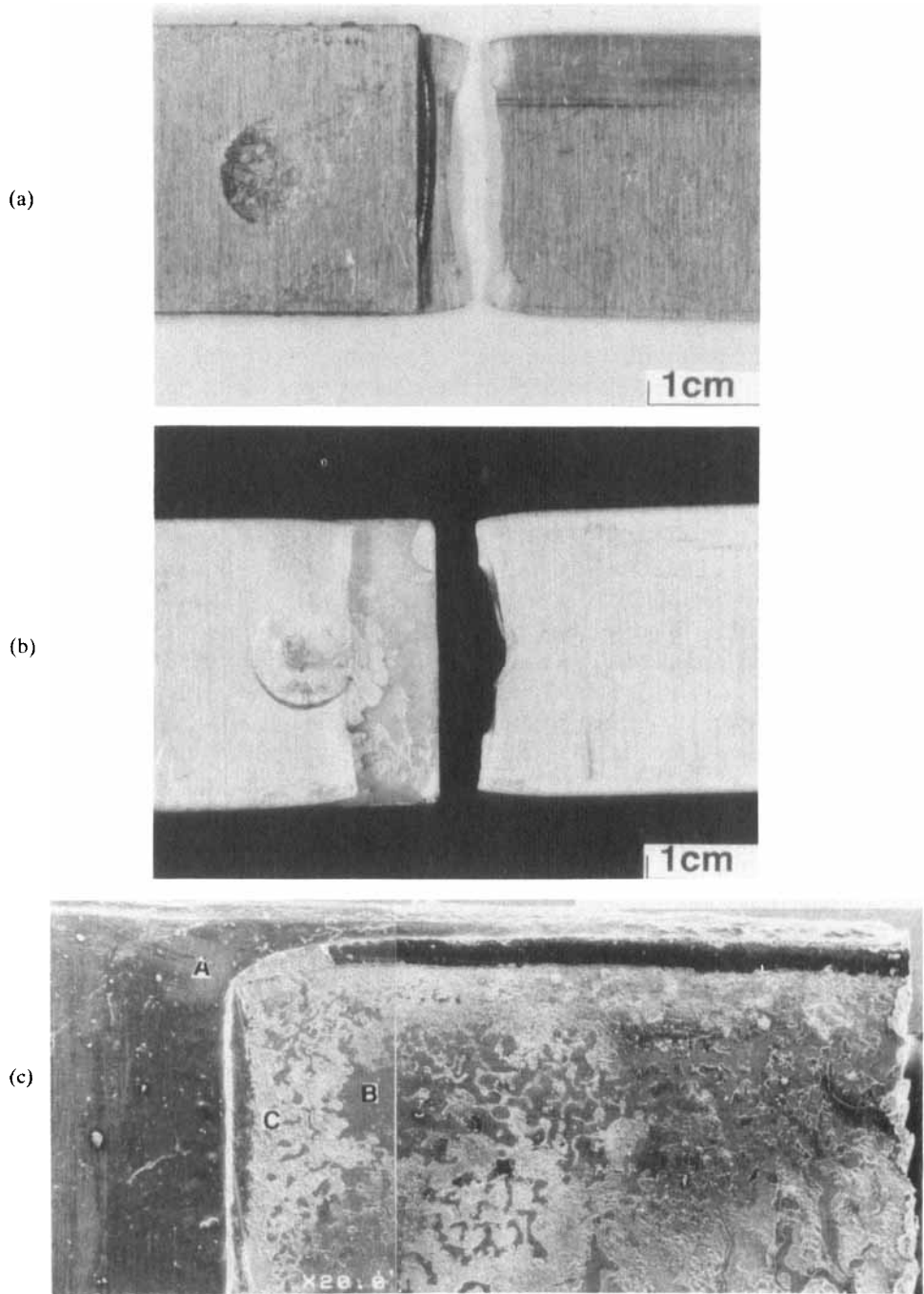


FIGURE 4 Failure modes at ambient condition: (a) adherend-tearing, (b) cohesive and nugget-tearing, and (c) scanning electron micrograph of a cohesive fracture surface.

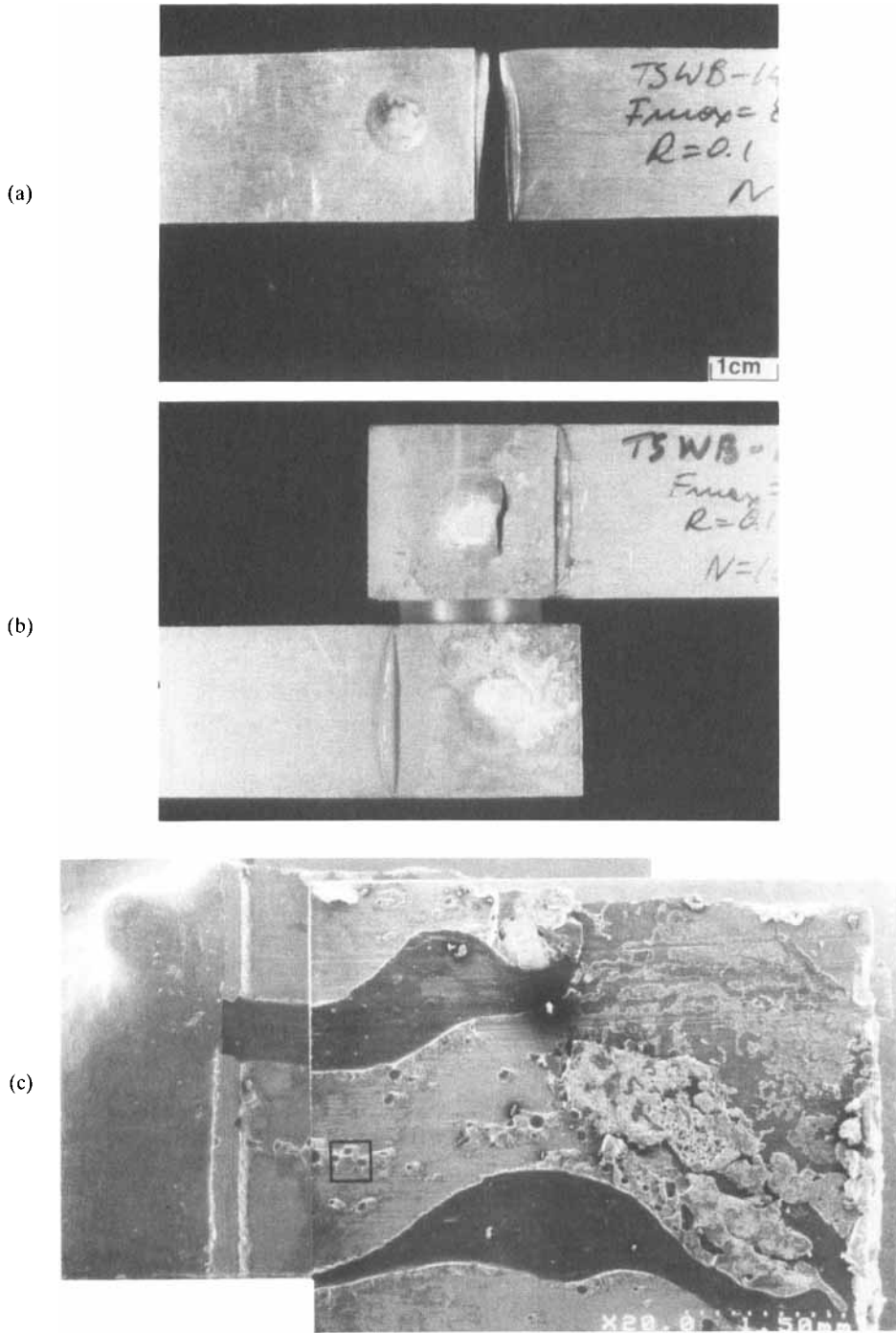


FIGURE 5 Fatigue failure mode in the 100% R.H./38°C: (a) adherend-tearing, (b) cohesive and nugget-tearing, (c) scanning electron micrograph of a cohesive failure mode, and (d) enlarged view of the region indicated by the square shown in (c).

(d)

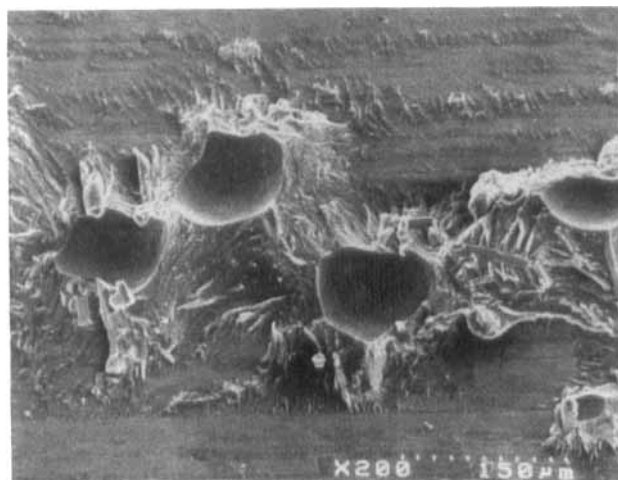


FIGURE 5 (Continued)

### Glass Transition Temperature ( $T_g$ ) of Bulk Adhesive

Figure 6 shows the DMA curves for shear storage ( $G'$ ) and loss ( $G''$ ) moduli as a function of temperature for dry (*i.e.*, ambient conditions) and wet (*i.e.*, 51 days exposure in 100% relative humidity at 38°C) specimens. Both specimens show the typical steplike drop in storage modulus and the peak in loss modulus characteristic of a glass transition. It can be seen that the modulus of the wet specimen is significantly lower than that of the dry specimen. Examination of the loss curves reveals that the  $T_g$  is approximately 30°C lower for the wet specimen than for the dry specimen. The depression of  $T_g$  is due to the water molecules diffusing into the adhesive.

The variations of moisture content and  $T_g$  with exposure time are shown in Figure 7. It is seen from Figure 7 that moisture content has not reached a "steady state" after about 51 days.

### Mechanism of Fatigue Strength Degradation

Two predominant mechanisms, plasticization<sup>12</sup> of adhesive and permanent weakening of the aluminum oxide,<sup>13</sup> have generally been proposed to explain the strength loss of adhesive-bonded joints in moisture and elevated temperature environments. In the former process, the durability of adhesive-bonded joints is controlled by the mechanical properties of the bulk adhesive, whereas in the latter process the interfacial failure between the adhesive and adherend is facilitated by weakening of the aluminum oxide. Since the fatigue life of weld-bonded aluminum in the 100% R.H. at 38°C environment is governed by crack initiation and growth from the adhesive, mechanisms for adhesive-bonded aluminum can also be applied to weld-bonded aluminum.

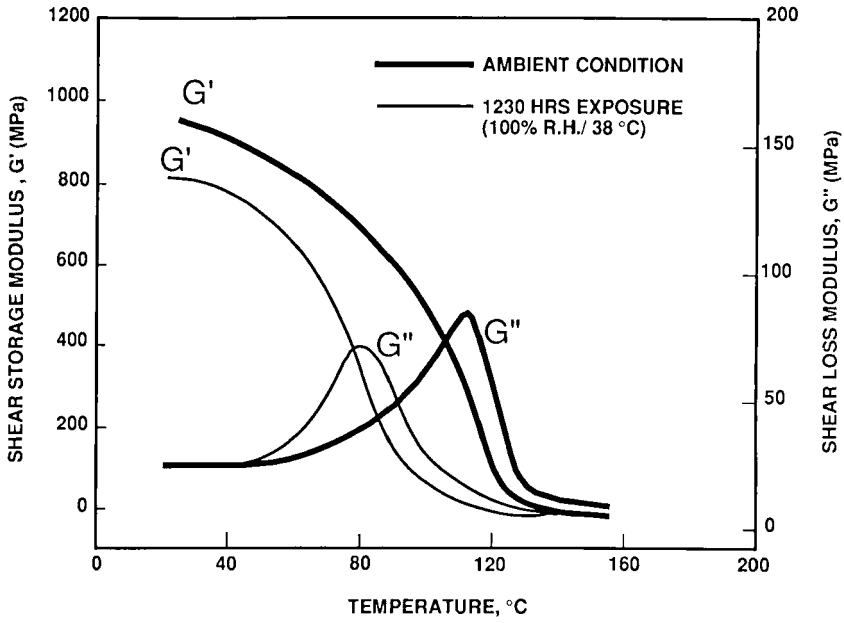


FIGURE 6 Dynamic shear storage ( $G'$ ) and loss ( $G''$ ) moduli of bis-phenol-A epoxy adhesive after exposure to ambient condition, and 100% relative humidity at 38°C (51 days).

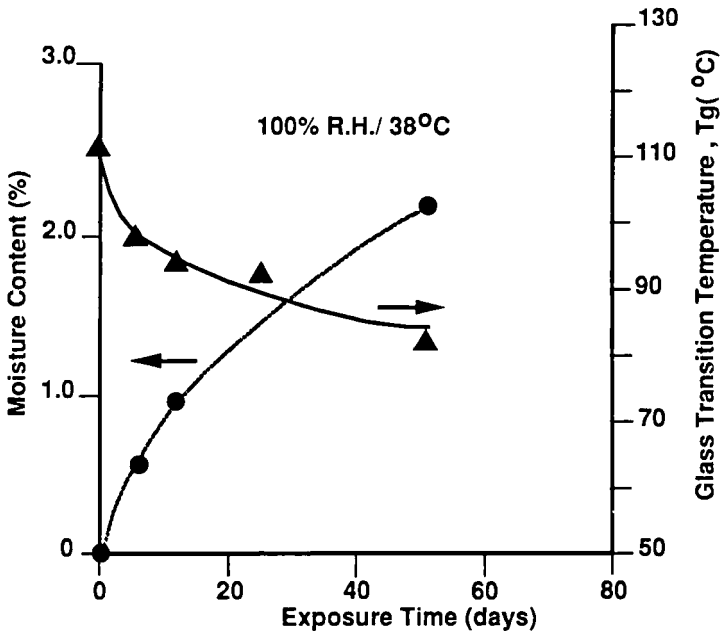


FIGURE 7 Moisture content and glass transition temperature,  $T_g$ , as a function of exposure cycle (100% R.H./38°C) of bis-phenol-A epoxy adhesive.

Downloaded At: 13:31 22 January 2011

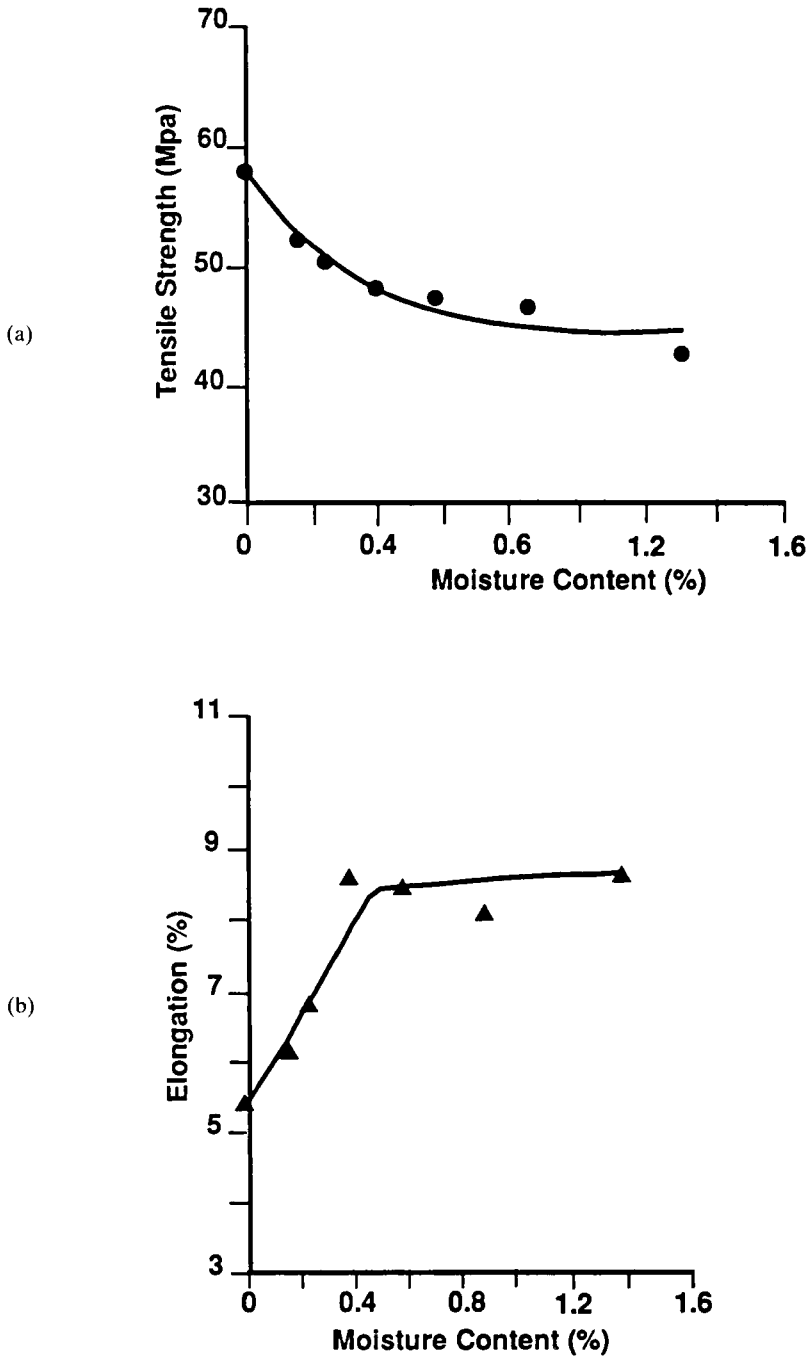


FIGURE 8 Effect of moisture content on the: (a) tensile strength, and (b) elongation of bis-phenol-A epoxy adhesive.

Downloaded At: 13:31 22 January 2011

In order to identify the failure mechanism, analysis of the properties of the surface is necessary. X-ray photoelectron spectroscopy (XPS) analyses of weld-bonded aluminum have been studied for dry and wet environments.<sup>14</sup> The binding energies of the aluminum (2p) peak were recorded. The aluminum (2p) peak occurred at binding energies characteristic of the trivalent state and showed no evidence for the presence of the aluminum hydroxide (or boehmite, AlOOH) on the surface of the wet weld-bonded aluminum. Therefore, we have ruled out the aluminum oxide weakening mechanism. The present results support that plasticization of the adhesive was a primary failure mechanism in the adhesive/aluminum joints investigated. The depression of the glass transition temperature ( $T_g$ ) shown in Figure 7, and the deterioration of tensile properties shown in Figure 8, are direct evidence of this. Each of these adhesive specimens, used to obtain Figure 8, was first placed in the environmental chamber for the required time and then tested right after removing from the chamber. The data in Figure 8 indicate that the tensile strength and elongation were affected appreciably by exposure to the moisture-saturated environment. The changes in tensile properties are undoubtedly due to the water absorption by the adhesive. The water absorption can be attributed to the moisture affinity of the highly polar functional groups in the adhesive. The phenylene-ether and hydroxyl groups which are present in all bis-phenol-A based epoxies can associate with water. On a molecular level the effect of water associating with the groups is to decrease the hydrogen bonding between polymer chains which, at the microscopic level, is reflected in a plasticization of the resin and a lowering of the  $T_g$ .<sup>15</sup> Moisture plasticizes the adhesive causing a lowering of the  $T_g$  which, in turn, adversely affects tensile properties. This degradation is enhanced by the combined action of the stress and elevated temperature.<sup>16</sup> The kinetics of the degradation process may be governed by the diffusion rate of the water vapor into the adhesive and the interaction rate of the water vapor and the adhesive material.

It is of interest to determine whether or not the changes in  $T_g$  (or tensile properties) of the adhesive are permanent. To answer this question, the  $T_g$  was measured of specimens which had been immersed for 12 hours in boiling water and then dried at 100°C for 6 hours prior to testing. The effect on  $T_g$  of moisture exposure followed by drying is shown in Table IV. As can be seen, by drying the adhesive, almost all of the loss in  $T_g$  is recovered. These results suggest that changes occurring in the adhesive during the moisture exposure are largely, although not 100%, reversible. Measurements of  $T_g$  of the adhesive after various exposures and drying cycles were

TABLE IV  
The effect of moisture and drying on the  $T_g$  of bis-phenol-A epoxy adhesive

Adhesive condition	Glass transition temperature, $T_g$ (°C)
As-Fabricated	112.1
12 hours in boiling water	74.6
12 hours in boiling water and then dried at 100°C for 6 hours	105.5

TABLE V  
Glass transition temperature ( $T_g$ ) of bis-phenol-A epoxy adhesive after various exposure cycles

Adhesive	Exposure cycle	$T_g$ (°C)
As-Fabricated	—	112.1
A <sub>1</sub>	6 days humidity exposure	98.2
A <sub>2</sub>	6 days humidity exposure and then dried in the ambient cond. for 80 days	88.8
B <sub>1</sub>	12 days humidity exposure	94.8
B <sub>2</sub>	12 days humidity exposure and then dried in the ambient cond. for 73 days	86.7
C <sub>1</sub>	25 days humidity exposure	93.2
C <sub>2</sub>	25 days humidity exposure and then dried in the ambient cond. for 117 days	87.5
D <sub>1</sub>	51 days humidity exposure	82.3
D <sub>2</sub>	51 days humidity exposure and then dried in the ambient cond. for 35 days	82.7

also carried out, and the results are given in Table V. Moisture content for a specimen after 51 days exposure in 100% R.H. at 38°C was 2.14%. If the specimen was exposed to the ambient conditions,  $T_g$  recovery would be anticipated. However, drying the adhesive in ambient conditions did not recover the  $T_g$ ; indeed, it may have caused a slight reduction in  $T_g$ . This result suggests that little water has been removed. Since water desorption rate is governed largely by the temperature, it would take a longer time to desorb water as the temperature decreases.

Examination of the specimen surfaces with SEM revealed that the adhesive with humidity exposure had minor micro-cavities (Fig. 9). These micro-cavities could be defects resulting from specimen fabrication or unequal swelling stresses developed in the bis-phenol-A epoxy and fillers from the water diffusion. Further study would be required to determine their exact cause. These micro-cavities may induce stress concentrations and result in crack propagation, leading to the joint failure. The loss in fatigue strength at  $5 \times 10^6$  cycles appeared to be due to the adhesive plasticization and micro-cavities which allowed the cracks to propagate more easily.

It is emphasized that the results presented in this paper only illustrate the reduction of fatigue strength of weld-bonded aluminum exposed to 100% R.H. at 38°C. The humidity level, temperature and loading conditions reported here are not simulative of a specific environment encountered by a vehicle. Furthermore, durability of weld-bonded aluminum may also depend upon the past history of the material (*i.e.*, adherend surface conditions and adhesive cure cycle). Nevertheless, the present results show that reduction of adhesive properties due to the moisture needs to be considered. Therefore, it is recommended that the adhesive properties used in vehicle structural design be adjusted to account for likely environmental effects. Long-term testing of the adhesive under service conditions should be correlated with accelerated tests to quantify design accommodation of environmental effects on structural performance.

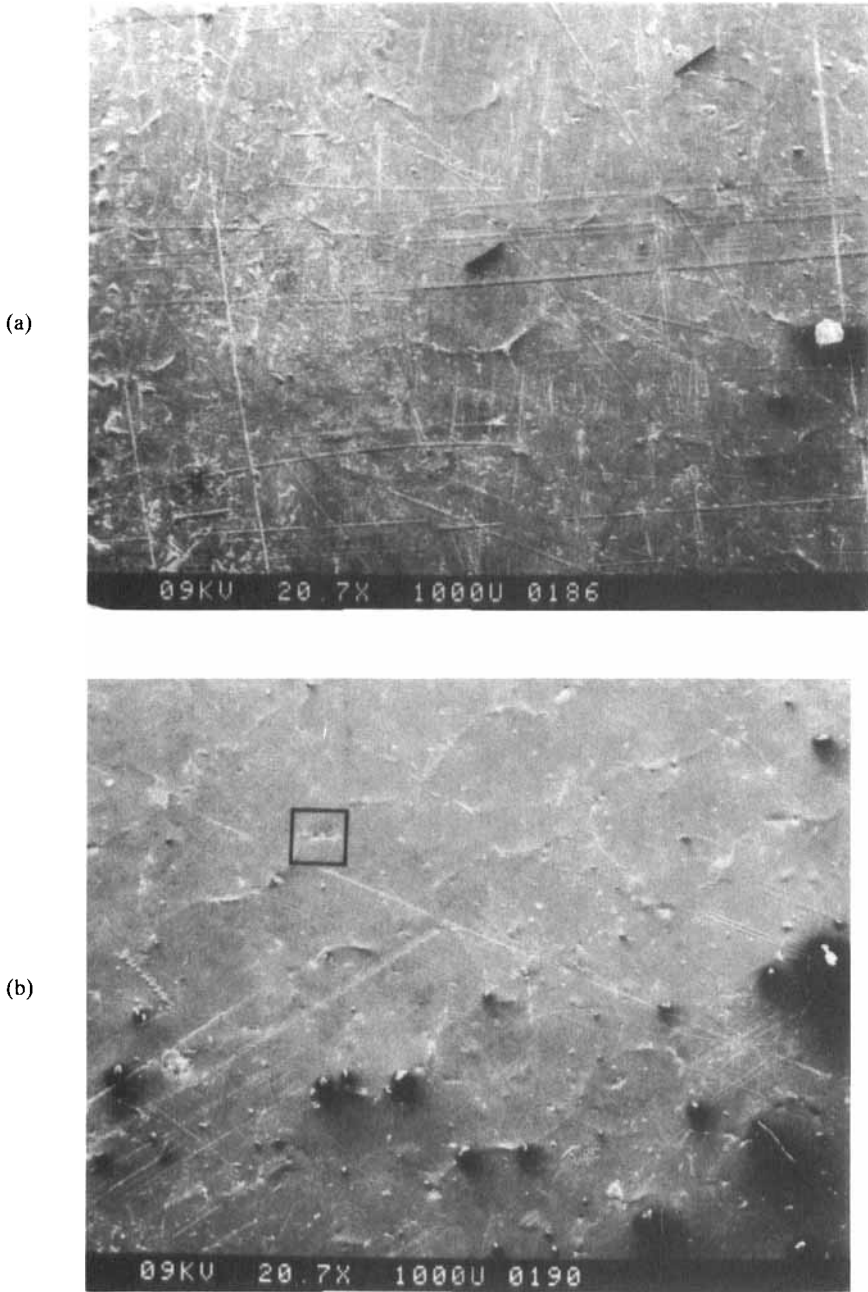
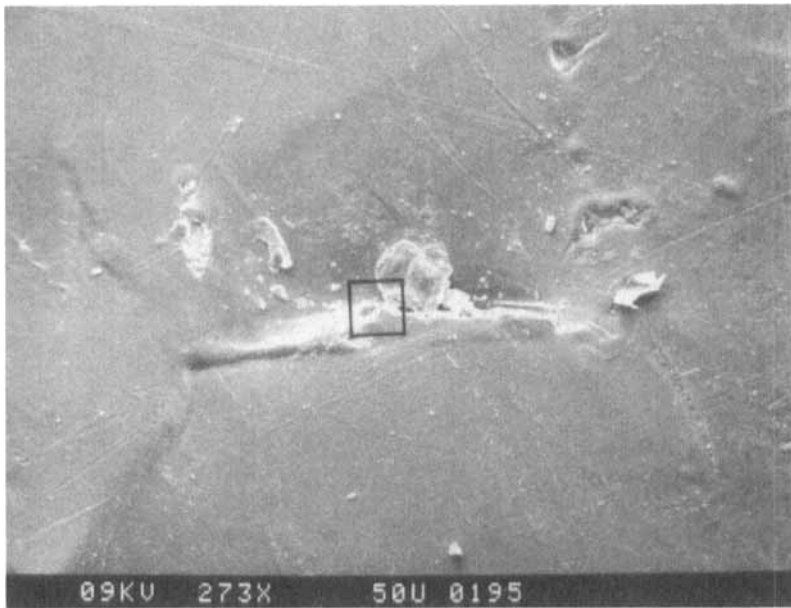


FIGURE 9 Scanning electron micrographs of bis-phenol-A epoxy adhesive surfaces: (a) as-fabricated, (b) 51 days exposure in 100% R.H./38°C, (c) and (d) enlarged view of the region indicated by the square shown in (b).

Downloaded At: 13:31 22 January 2011



(c)



(d)

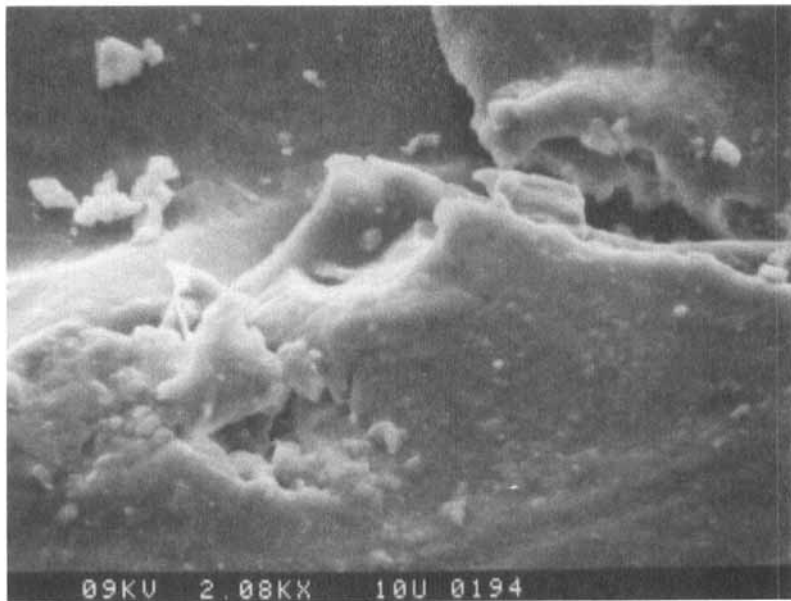


FIGURE 9 (Continued)

## CONCLUSIONS

1. The presence of moisture (100% R.H.) at 38°C decreases the fatigue strength of weld-bonded aluminum joints; the degree of reduction is more pronounced in the high-cycle regime (*i.e.*, 33% loss in fatigue strength at  $5 \times 10^6$  cycles).
2. Moisture plasticizes the bis-phenol-A epoxy adhesive causing a lowering of the glass transition temperature  $T_g$  which, in turn, reduces the tensile properties.
3. Plasticization of the adhesive is responsible for fatigue strength reduction of weld-bonded aluminum in the humid environment.
4. A cohesive failure mode was observed both for dry (ambient condition) and wet (100% R.H. at 38°C) weld-bonded aluminum. Moisture caused the locus of failure to shift from the adhesive layer (in dry specimens) to the regions near the aluminum-adhesive interface (in wet specimens).
5. The moisture-induced change in glass transition temperature of bis-phenol-A epoxy adhesive is essentially reversible.

## Acknowledgments

The authors would like to express their great appreciation to Drs. G. Banas and F. V. Lawrence, Jr. for performing the fatigue experiments.

## References

1. N. Chessin and V. Curran, "Preparation of aluminum surfaces for bonding," *Applied Polymer Symposia* **3**, 319–325 (1966).
2. G. E. Nordmark, "Fatigue performance of aluminum joints for automotive application," SAE Paper 780397 (1978).
3. J. D. Minford, *Treatise on Adhesion and Adhesives*, Vol. 5, R. L. Patrick, Ed. (Marcel Dekker, New York, 1981), p. 45.
4. P. C. Wang, P. Frechette, M. Balogh, C. Wong, M. Myers and D. McEwen, "Identification and analysis of bis-phenol-A epoxy adhesive," Unpublished work (1992).
5. *Engineering Materials Handbook*, Vol. 1 (ASM International, Metals Park, Ohio, 1987), p. 779.
6. A. H. Bowker and G. J. Lieberman, *Engineering Statistics* (Prentice-Hall, Englewood Cliffs, N.J., 1972).
7. J. A. Davidson, "Design-related methodology to determine the fatigue life and related failure mode of spot-welded sheet steels," Conf. *Proceedings of International Conf. on Technology and Applications of HSLA Steels*, 539–551 (1983).
8. K. F. Glaser and G. E. Johnson, "Construction experience on aluminum experimental bodies," SAE paper 740075 (1974).
9. J. A. Laird, "Glass surface chemistry for glass reinforced plastics," Final report, Navy contract W-0679-C(FBM), NTIS: AD-413 977 (1963).
10. P. C. Wang, "Three-dimensional finite element stress analyses of weld-bonded joint," Unpublished work, General Motors Research Laboratories (1991).
11. G. E. Dieter, *Mechanical Metallurgy* (McGraw-Hill Inc., New York, 1976).
12. J. C. Mcmillan, *Development in Adhesives-2*, A. J. Kinloch, Ed. (Applied Science Publishers, London, 1981), p. 243.
13. G. D. Davis and J. D. Venables, in *Durability of Structural Adhesives*, A. J. Kinloch, Ed. (Applied Science Publishers, London, 1983), p. 71.
14. P. C. Wang and S. Gaarenstroom, "Mechanism of the hygrothermal attack of weld-bonded aluminum," to be published (1993).
15. R. De Iasi and J. B. Whiteside, *Advanced Composite Materials, ASTM STP 658* (1978).
16. S. N. Zhurkov and V. E. Korsukov, "Atomic mechanism for the destruction of stressed polymer," *Sov. Phys. Solid State*, **15**(7), 1379–1384 (1984).